Articles

Synthesis, Characterization, and Photovoltaic Properties of Novel Semiconducting Polymers with Thiophene−Phenylene−Thiophene (TPT) as Coplanar Units

Shu-Hua Chan, Chih-Ping Chen, Teng-Chih Chao, Ching Ting, Chin-Sheng Lin, and Bao-Tsan Ko*

Materials and Chemical Laboratories, Industrial Technology Research Institute, 195, Sec. 4, Chung Hsing Road, Chutung, Hsinchu, 310, Taiwan

Received March 5, 2008; Revised Manuscript Received June 6, 2008

ABSTRACT: Four novel conjugated polymers (**P1**, **P2**, **P3**, and **P4**) based on coplanar thiophene−phenylene−thiophene (TPT) derivatives have been designed and synthesized for application in polymer solar cells (PSCs). The optical, electrochemical, field effect carrier mobility, and photovoltaic properties of **P1**−**P4** are investigated and compared with those of poly(3-hexylthiophene) (P3HT). PSCs are fabricated based on the blend of the polymers and [6,6]-phenyl-C61-butyric acid methyl ester ($PC_{61}BM$) or 1-(3-methoxycarbonyl)propyl-1-phenyl-[6,6]-C-71 ($PC_{71}BM$) with a weight ratio of 1:3. The maximum power conversion efficiency (PCE) of the PSCs based on **P3**/$PC_{71}BM$ system reaches 3.3% with a short circuit current density (J_{sc}) of 7.6 mA/cm^2, an open circuit voltage (V_{oc}) of 0.8 V, and a fill factor (FF) of 0.54 under AM 1.5G (100 mW/cm^2) illumination. The results indicate that the coplanar TPT conjugated derivatives are promising PSC materials.

1. Introduction

Environmental issues such as fossil fuel shortage and global warming have gained worldwide acknowledgment, and the need for clean renewable energy becomes more urgent as we enter the 21th century. Among all renewable energy sources, solar energy, which is clean, abundant, and virtually limitless, has been extensively studied in recent years. Polymer-based photovoltaics[1] being one of the third-generation solar cell technology offers advantages of lightweight, high-throughput manufacture, and environmentally benign for portable energy applications. It is also expected that the power generation cost of this technology can be as low as US$ 1.0/Wp should the high-throughput process be introduced in the future. Since the pioneering works of A. J. Heeger and co-workers in 1995,[2] the power conversion efficiency (PCE) of the polymer solar cell (PSC) has achieved significant improvement due to the introduction of the so-called bulk-heterojunction (BHJ) concept, where a photoactive layer consists of an interpenetrating network of π-conjugated polymer donors and soluble fullerene or nanocrystal acceptors. The most successful system until now is a blend of regioregular poly(3-hexylthiophene) (rr-P3HT) and [6,6]-phenyl-C61-butyric acid methyl ester (PCBM), in which the well-acknowledged state-of-the-art P3HT/PCBM BHJ solar cells give efficiencies in the range of 4−5%.[3] The efficiencies of polymer solar cells can in theory be further improved through careful engineering of both materials and device structures. While the best performing solar cells can thus far be achieved based on the BHJ concept, new devices' architecture design and fabrication process should be optimized in order to control the morphology of the active layer, reduce bulk or interface resistance, and enhance carrier transportation. On the other hand, key issues for material engineering includes ease of processibility, effective light harvesting (such as low-bandgap semiconducting polymer[4] with broad absorption and high absorptivity), and high carrier mobility property. However, it is more challenging to improve the charge mobility of the conjugated polymers in comparison with improving their absorption properties.

To increase the hole mobility of the polymers, other than increasing molecular weight and decreasing polydispersity of polymers,[5] enhancing $\pi-\pi$ stacking of the polymer backbone and to produce highly organized morphology by either side chain self-assembly[6] or introduction of more rigid planar monomer to form liquid-crystalline phase structure[7] have been proven to be effective approaches. PBTTT,[7] thiophene−thiazolothiazole copolymers,[8] and benzodithiophene copolymers[9] have been reported that by incorporating fused aromatic units into the polymer backbone can achieve high field effect carrier mobility up to 0.1−0.8 cm^2/(V s). The presence of rigid fused ring is expected to enhance the rigidity of the molecular backbone and enhance the degree of conjugation,[10] and can also benefit to avoid possible "chain folding", which may limit the charge carrier mobility of semiconducting polymers at higher molecular weights.[11] Recently, Wong et al. have designed and synthesized a novel coplanar chromophore that feature phenylene ring(s) fused to thiophene, namely, phenylene−thiophene−phenylene (TPT) derivatives.[12] The molecular configurations of the π-conjugated backbones are confirmed through X-ray crystallography, and the heteroarene-fused molecular frameworks of the TPT unit exhibit nearly coplanar conformations. In this paper, we present a series of novel coplanar semiconducting polymers, which are the first new class of copolymers utilizing a TPT derivative as the fused coplanar unit in the polymer chain. Those also show improved charge-transport properties with field effect hole mobility up to 3×10^{-3} cm^2/(V s) as well as suitable

* Corresponding author. E-mail: BTKo@itri.org.tw. Tel: 886-35-91493. Fax: 886-35-827694.

10.1021/ma800494k CCC: $40.75
Published on Web 07/08/2008

Scheme 1. Synthetic Routes of the Monomers and Polymers[a]

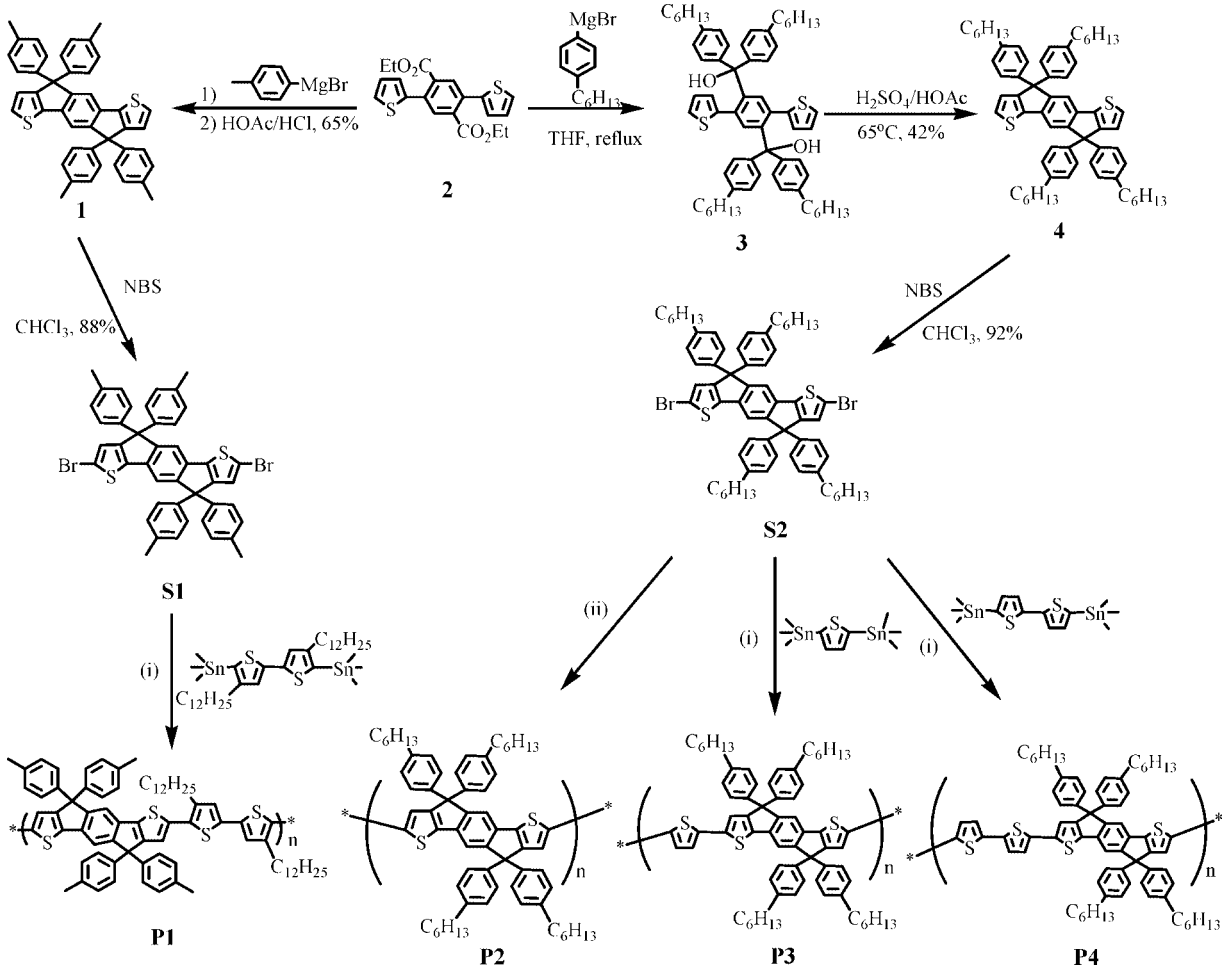

[a] (i) Stille coupling polymerization: tris(dibenzylideneacetone)dipalladium/tri(*o*-tolyl)phosphine, chlorobenzene, microwave heating, 30 min. (ii) Yamamoto coupling polymerization: $Ni(COD)_2$, toluene/DMF, 60 °C, 2 d.

electronic energy levels and good processability for PSC application. The combination of these properties allowed the best PSC efficiencies up to 3.3% while blended with $PC_{71}BM$, with a short circuit current density (J_{sc}) of 7.6 mA/cm^2, an open circuit voltage (V_{oc}) of 0.8 V, and a fill factor (FF) of 0.54 under AM 1.5G (100 mW/cm^2).

2. Results and Discussion

2.1. Material Synthesis and Structural Characterization. The synthetic routes of monomers (**S1** and **S2**) and polymers are outlined in Scheme 1. *p*-Thiophene−phenylene−thiophene derivative (**1**, *p*-TPT) was synthesized by following the previous literature of Wong's group.[12] Bromination of **1** by *N*-bromosuccinimide (NBS) gave the dibromo monomer **S1** in high yield. In order to improve solubility of subsequently synthesized conjugated polymers, alkyl side chains that incorporated *p*-TPT derivative were designed and developed. The addition of excess amounts of 4-hexylaryl Grignard reagent, which were prepared in advanced from 4-bromohexylbenzene, onto the ester group of compound **2** gave the corresponding alcohol **3**. Without further purification, compound **3** was then treated to acid-mediated intramolecular annulation to afford the tetrahexyl substituent TPT (**4**) in 42% yield. Again, **4** was brominated by NBS to obtain the corresponding dibromo monomer **S2**. The structures of **S1** and **S2** were confirmed by ^{1}H NMR, ^{13}C NMR, and elemental analysis, and the data are included in the Experimental Section. The ^{1}H NMR spectra of **S1** and **S2** are shown in Figure 1, where all the peaks are assigned to their corresponding hydrogen atoms based on chemical shift, integral area, and coupling constant.

Copolymers **P1**, **P3**, and **P4** were synthesized by Pd(0)-catalyzed Stille coupling polymerization in chlorobenzene under microwave heating condition. Homopolymer **P2** was synthesized by Yamamoto's coupling polymerization in the presence of excess $Ni(COD)_2$ in toluene/DMF mixing solvent at 60 °C for 2 days. All the polymers except **P2** were completely soluble in organic solvents such as chloroform ($CHCl_3$), toluene, tetrahydrofuran (THF), and chlorobenzene. **P2** was partly soluble in $CHCl_3$ probably due to high molecular weight. Fraction of **P2** could be extracted by $CHCl_3$ to collect $CHCl_3$-soluble portion. The weight-average molecular weights (M_w) of **P1**, $CHCl_3$-soluble **P2**, **P3**, and **P4** were determined by gel permeation chromatography (GPC) against polystyrene standards in THF eluent and were found to be in the range of 21 800−48 700 with a polydispersity index (M_w/M_n) of 1.52−2.19 (Table 1).

All the polymers exhibited good thermal stability with 5% weight-loss temperature (T_d) higher than 300 °C under N_2, as revealed by thermogravimetric analysis (TGA) (see Figure 2). The thermal analyses of all the polymers were also investigated by differential scanning calorimetry (DSC). **P2**, **P3**, and **P4** showed a glass transition temperature (T_g) of 112, 95, and 105 °C, respectively, and no crystallization (T_c) and melting transition temperatures (T_m) up to 300 °C. However, T_g and T_m of **P1** were not observed in the range of 40−300 °C.

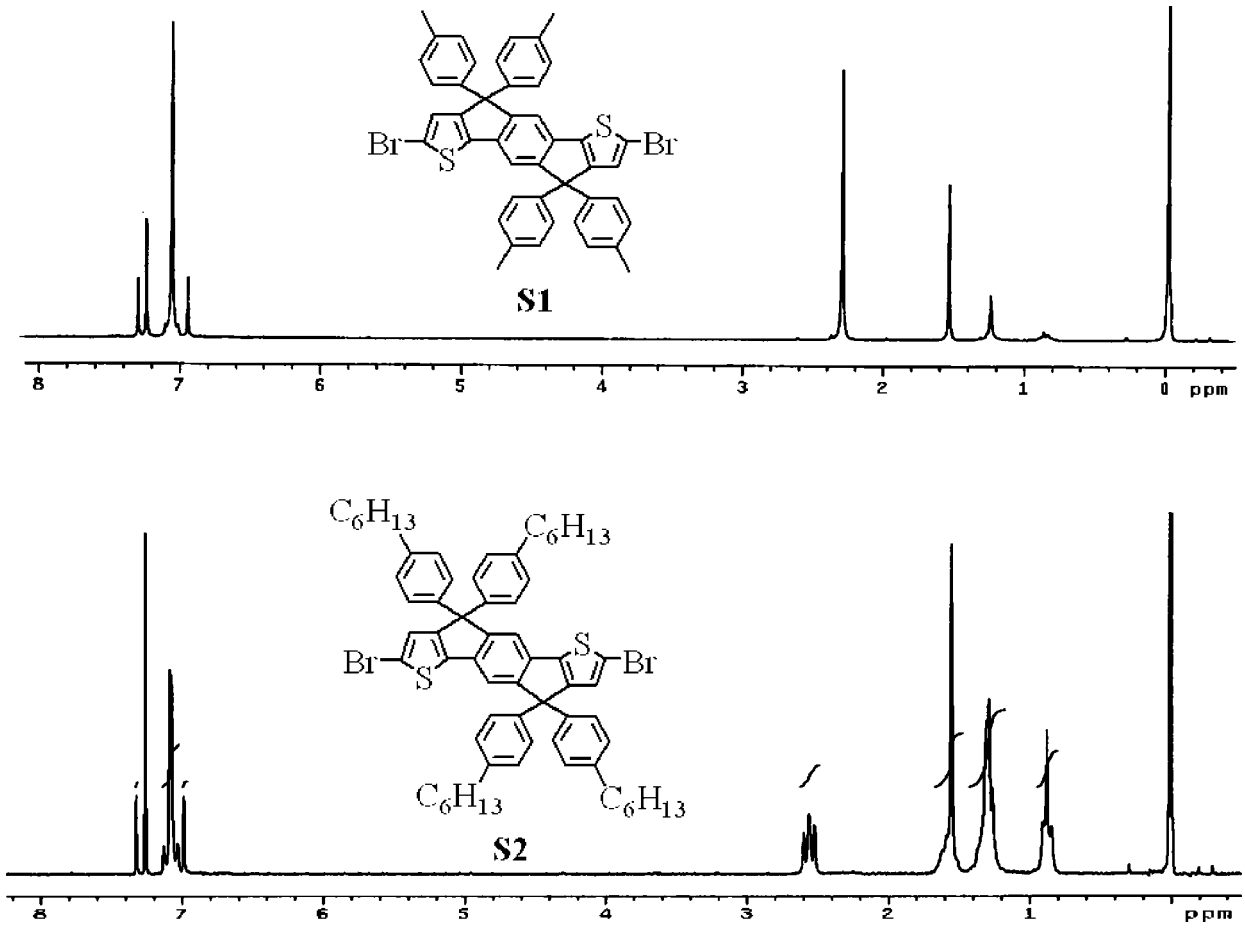

Figure 1. ^{1}H NMR spectra of monomer **S1** and **S2**.

Table 1. Molecular Weights, FET Mobility, and Optical and Electrochemical Properties of Various Polymers

	M_w (PDI)	λ_{max} (film)	α^a (cm^{-1})	E_g^{opt} (eV)	E_{ox} (V)^b	IP (eV) (HOMO)	EA (eV) (LUMO)	μ_h^c ($cm^2/(V\ s)$)	on/off^c
P1	25200 (1.52)	490	6.3×10^5	2.10	0.71	5.17	3.07	3.7×10^{-4}	5.2×10^3
P2	21800 (1.97)	510	3.0×10^5	2.10	0.72	5.18	3.08	1.5×10^{-4}	1.4×10^4
P3	48700 (2.19)	510	9.9×10^5	2.08	0.64	5.1	3.02	8.3×10^{-4}	9.1×10^4
P4	29300 (1.87)	508	9.4×10^5	2.11	0.72	5.18	3.07	3.0×10^{-3} (9.9×10^{-4})^d	1.3×10^6 (6.5×10^5)^d
P3HT	47000 (2.45)	552	1.2×10^6	1.90	0.74	5.20	3.30	6.5×10^{-2}	1.3×10^3

^{a} Absorption coefficient was determined at λ_{max} in THF. ^{b} E_{ox} is the onset potential of oxidation of polymer. ^{c} Thin-film FETs were fabricated from 1 wt % *o*-DCB solutions. ^{d} $CHCl_3$ solvent was used instead of *o*-DCB.

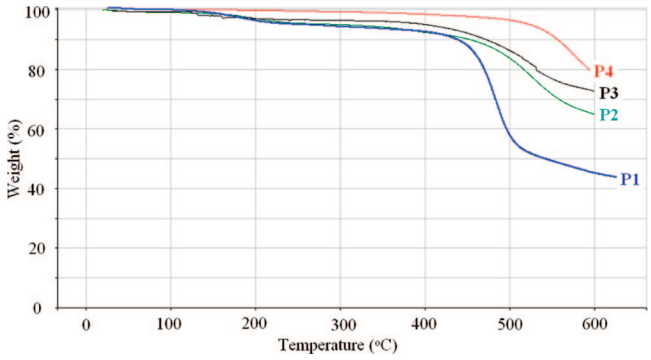

Figure 2. TGA thermograms of **P1**−**P4** in N_2.

The molecular structures of the polymers were verified by ^{1}H NMR and UV−vis spectra. ^{1}H NMR spectrum of **P1**, **P2**, and **P4** are shown in Figure 3 for comparison. The characteristic peaks at δ 7.40−7.00 ppm can be assigned to the resonance of protons on the thiophene ring, phenylene ring, and phenyl side chain groups. The peaks in the ranges of δ 2.80−0.80 ppm arise from alkyl substituents (−CH_3 or −$C_{12}H_{25}$ or −C_6H_{13}), and the peak area integral ratio between the aromatic and aliphatic signals agrees with the corresponding molecular structure of the polymers.

2.2. Optical Properties. The UV−vis absorption spectrums of **P1**−**P4** films are shown in Figure 4, and the corresponding maximum absorption wavelengths (λ_{max}) are summarized in Table 1. The λ_{max} of **P2**−**P4** are all around 510 nm and that of **P1** shows slight blue-shift λ_{max} = 490 nm). The optical bandgaps (eV) of **P1**−**P4** estimated from the absorption edge are almost the same, ~2.1 eV, which is very similar to that of the common PSC used conjugated polymer, poly(2-methoxy-5-{3′,7′-dimethyl-octyloxy}-*p*-phenylenevinylene) (MDMO-PPV). An additional attractive characteristic of **P3** and **P4** is that they have high absorption coefficient in comparison to the well-known regioregular P3HT polymer. The dilute concentrations of those polymers solution in THF are made to be the same and their absorption coefficient (α) could be calculated from Beer's law equation. As shown in Figure 5, **P3** and **P4** display similar value (~10^6 cm^{-1}) at λ_{max} (~510 nm) and both of whose values are comparable to that of P3HT (~1.2×10^6 cm^{-1}) at λ_{max} (~450 nm). However, **P1** and **P2** exhibit significantly lower absorption coefficient than the other polymers. The solid film photoluminescence of the polymer (**P3**) lies near the yellow region with

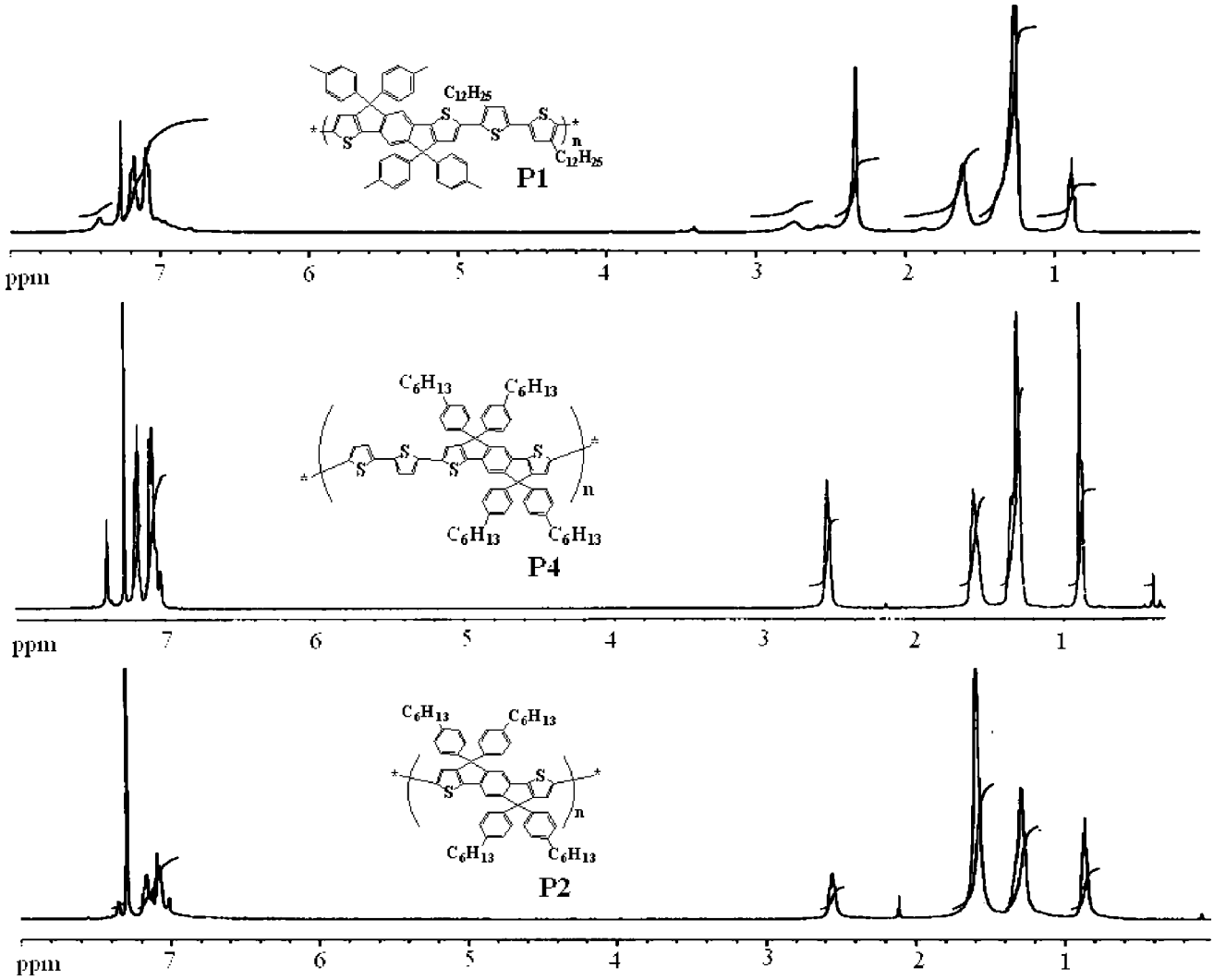

Figure 3. ^{1}H NMR spectra of **P1**, **P2**, and **P4** in $CDCl_3$.

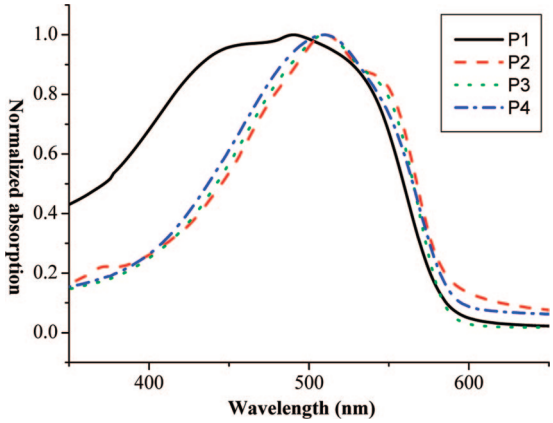

Figure 4. UV−vis absorption spectra of the polymer films.

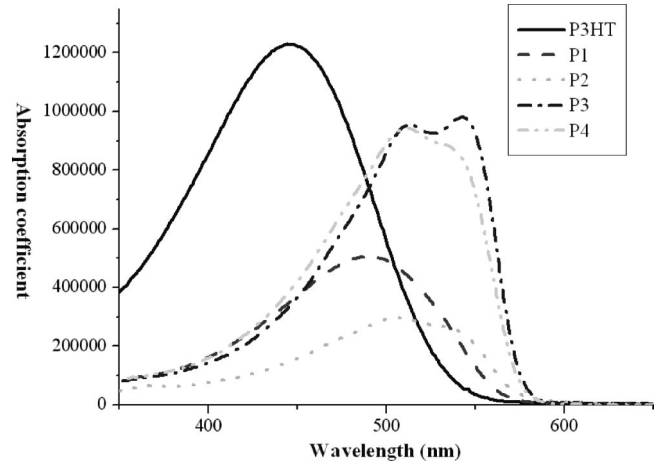

Figure 5. UV−vis absorption spectra of the polymer solutions in THF and their absorption coefficients calculated from Beer's law.

a maximum of emission at 576 nm and is almost completely quenched by the addition of PCBM with from 1:1 to 1:3 weight ratio (Figure 6). This highly efficient photoluminescence quenching is the result of ultrafast photoinduced charge transfer from the polymer to PCBM. On the basis of all the above optical measurements, we can assume that **P3** and **P4** are suitable candidates for applications in PSCs.

2.3. Electrochemical Properties. Cyclic voltammograms demonstrate that the onset oxidation potentials of **P1**−**P4** are all similar with that of P3HT. Moreover, the HOMO and LUMO levels of **P1**−**P4** could also be calculated in combination of results of the electrochemical and optical properties as summarized in Table 1.

2.4. Hole Mobility from Field Effect Transistor Characteristics. The field-effect carrier mobilities of the coplanar semiconducting polymers were investigated by fabricating and evaluating thin film field-effect transistors (FETs) based on the

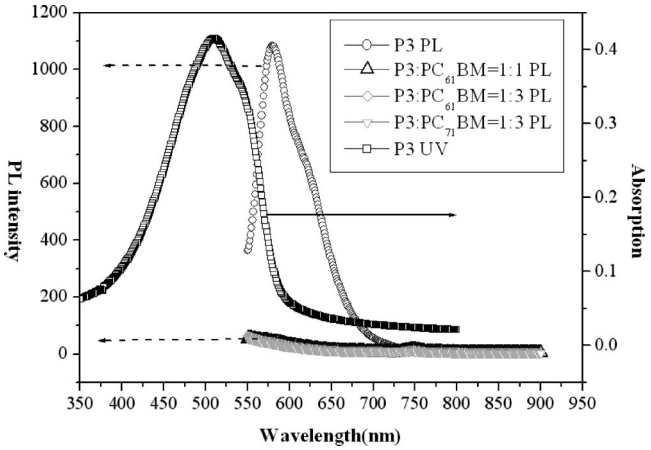

Figure 6. UV−vis spectrum in the solid state (□) and photoluminescence in the solid state (○) of **P3** and photoluminescence quenching for **P3**:$PC_{61}BM$ with 1:1, 1:3 (△, ◇) and **P3**:$PC_{71}BM$ with 1:3 weight ratio (▽).

bottom contact geometry (Figure 7a) similar to the previous literature.[13] Figure 7b displays the plots of source−drain current (I_{DS}) as a function of source−drain voltage (V_{DS}) at different gate voltages (V_G) from 0 to −40 V. On the application of negative V_G, characteristic transistor behavior was observed, indicating that the fabricated FET had p-channel characteristics. As the V_{DS} increases, the current I_{DS} approached into the saturation regime and could be described by eq 1:

$$I_D = (W/2L)C_0\mu(V_G - V_T)^2 \quad (1)$$

where μ is the field-effect hole mobility, W is the channel width (1000 μm), L is the channel length (10 μm), C_0 is the capacitance per unit area of the gate dielectric layer (SiO_2, 100 nm, C_0 = 34.5 nF/cm^2), and V_T is the threshold voltage. The saturation region field-effect mobility was thus calculated from the transfer characteristics of the OFETs involving plotting $I_D^{1/2}$ vs V_G. In a typical case, OFET of **P4** was made by spin-coating a 1.0 wt % polymer solution in $CHCl_3$ or *o*-dichlorobenzene onto n-doped Si/SiO_2 substrates and dried for 1 h at 150 °C. In order to promote the molecular chain ordering of the polymer semiconductor at the gate dielectric/semiconductor interface, the gate dielectric surface was modified by the silylating agent hexamethyldisilazane (HMDS). The output and transfer characteristics of **P4** FETs processed from dichlorobenzene are shown in Figure 7c. **P4** devices show typical p-channel FET characteristics with good drain-current modulation and well-defined linear and saturation regions. A field-effect hole mobility of 9.9×10^{-4} cm^2/(V s) and an on/off ratio of 6.5×10^5 are observed in **P4** FETs processed from $CHCl_3$. A slight improvement in hole mobility to 3.0×10^{-3} cm^2/(V s) and better on/off ratios (1.3×10^6) can be obtained in **P4** FETs processed from the higher-boiling dichlorobenzene (DCB) solutions. OFETs processed from DCB also indicates much lower threshold voltages ($V_T = -0.4$ V) compared to those processed from $CHCl_3$ ($V_T = -2.9$ V), suggesting that **P4** devices from DCB have more ordered polymer chains that diminish structural disorder at the polymer/dielectric interface. Furthermore, FETs from the other copolymers (**P1**−**P3**) have similar or lower performances in comparison to **P4** FETs as shown in Table 1.

2.5. Photovoltaic Properties. According to the optoelectronic properties described above, these coplanar semiconducting polymers are suitable materials in polymer photovoltaic applications. The photovoltaic cells were fabricated by spin-coating from a dichlorobenzene (DCB) solution of polymer/PCBM blend. Polymeric bulk-heterojunction solar cells (glass/ITO/PEDOT:PSS/polymer:PCBM/Ca/Al) were fabricated using a method similar to that in the previous report.[14] Because PSC performance is known to have strong dependency of donor/acceptor ratio and the thickness of active layer, a series of devices were fabricated adopting a variety of thickness and polymer/PCBM ratio. The better fabrication conditions were obtained from a 10 mg/mL DCB solution, 1000 rpm of spin-coating rate and polymer/PCBM ratio of 1:3 (w/w). Table 2 shows the output characteristics of the various polymer devices. The performance of P3HT device is comparable with previous reported data under similar condition.[3] The optimum efficiency is around 3.9%, prepared from a 17 mg/mL (P3HT:PCBM = 1:1 w/w) DCB solution. Unlike the P3HT system, the best composition of TPT polymers to PCBM ratio is more like the MDMO-PPV/PCBM system.[15] Lower content of PCBM (<67 wt %) leads to inefficient electron−hole separation and non-suitable morphology. With increasing PCBM contents, both the J_{sc} and FF increase in our TPT polymers devices. A better example to illustrate the photovoltaic performance of blending device is found to be the **P3**/PCBM system. Figure 8a shows $I-V$ characteristics for the devices made by **P3** either with $PC_{61}BM$ or $PC_{71}BM$, respectively. The best performance of PSC was fabricated by **P3**/$PC_{71}BM$ which reaches an AM 1.5G power conversion efficiency (PCE) of 3.3%, with a short circuit current density (J_{sc}) of 7.6 mA/cm^2, an open circuit voltage (V_{oc}) of 0.8 V, and a fill factor (FF) of 0.54. In comparison to the device based on P3HT/$PC_{61}BM$, the PCE of **P3**/$PC_{71}BM$ (3.3%) is about 15% lower than the P3HT device (3.9%). Figure 8b compares the incident photon-to-current conversion efficiency (IPCE) spectra of devices fabricated with P3HT and **P3** materials. The P3HT device shows the typical spectral response with a maximum IPCE of 63% at 540 nm, similar to the previous studies.[3c,4c] The shape of the IPCE curve of the **P3** device is consistent with UV−vis spectrum of **P3**/$PC_{71}BM$ blend film (Figure 8d) with the IPCE maximum being approximately 49% at 500 nm. Hence, the lower photocurrent of **P3** device compared to the P3HT device is partially due to the limited absorption at the long-wavelength range. Figure 8c shows AFM image of **P3**/$PC_{71}BM$ blend film fabricated at the optimized conditions. No indication of a large-scale phase separation is observed as other blend films often show. The root mean squares (rms) of the film roughness, however, are as low as 0.8 nm. The PCEs of **P3**/$PC_{61}BM$ devices are lower in comparison with those of **P3**/$PC_{71}BM$, which is due primarily to a remarkable decrease in current density while V_{oc} and FF are comparable. As can be seen in Figure 8d, the significantly lower J_{sc} is probably caused by the limited absorption range of the **P3**/$PC_{61}BM$ device. The presence of $PC_{71}BM$ can provide more photon current because it can absorb the photon beyond wavelength of 600nm. The device performances of **P4**/PCBM show the same tendency in our experiments.

The other TPT derivatives show varied performance in PSC as shown in Table 2. The significantly lower PCEs of the corresponding derivatives, **P1**, is due to lower values for both J_{sc} and FF while V_{oc} remains in the higher range from 0.76 to 0.8 V. On the other hand, the low J_{sc} value obtained by **P2** is due to its lower absorption coefficient. Moreover, devices made with **P1** showing a lower FF than other polymers makes us suspect that the **S2** can provide better interaction with PCBM than **S1** moiety. However, more evidence is required to carefully check the findings and assumption for TPT derivatives in the future.

3. Conclusion

In conclusion, we have demonstrated a series of novel TPT derivatives incorporated semiconducting polymers. The absorption spectral, electrochemical, field effect hole mobility, and photovoltaic properties of **P1**−**P4** were investigated and com-

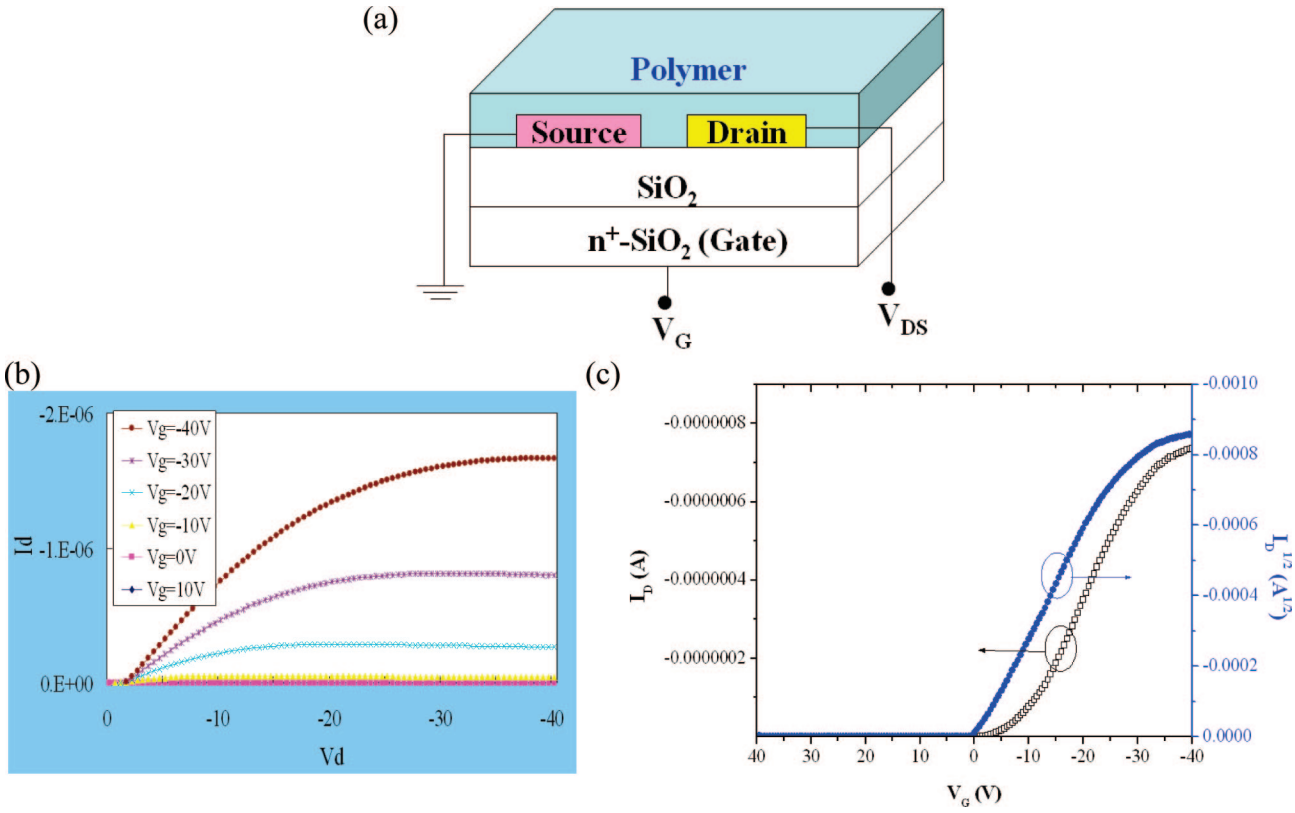

Figure 7. (a) Schematic illustration of the bottom-contact field-effect transistor (FET) based on **P4**. The source and drain electrodes consist of Pt contact. (b) Source−drain current (I_{DS}) vs source−drain voltage (V_{DS}) output characteristics of the device. (c) Transfer characteristics of the same device taken at $V_{DS} = -40$ V.

Table 2. Characteristic Current−Voltage Parameters from Device Testing at Standard AM 1.5G Conditions

	polymer/PCBM (w/w ratio)	J_{sc} (mA/cm^2)	V_{oc} (V)	FF	η (%)
P3HT[a]	1:1[b]	9.9	0.64	0.62	3.9
P1	1:3[b]	3.5	0.79	0.39	1.1
P2	1:3[b]	1.4	0.76	0.54	0.6
P3	1:2[b]	4.8	0.79	0.53	2.0
P3	1:3[b]	5.3	0.77	0.53	2.2
P3	1:3[c]	7.6	0.80	0.54	3.3
P4	1:2[b]	4.1	0.75	0.45	1.4
P4	1:3[b]	4.6	0.76	0.49	1.7
P4	1:3[c]	7.0	0.79	0.49	2.7

[a] Purchased from Rieke-Metal (4002E series). [b] Using $PC_{61}BM$ (purchased from Nano-C) as acceptors. [c] Using $PC_{71}BM$ (purchased from Solenne) as acceptors.

pared to those properties of P3HT. Photovoltaic cells based on these polymers blend with $PC_{71}BM$ acceptor have the highest power conversion efficiency of 3.3%. These polymers demonstrate a new family of conjugated polymer along the path toward achieving a low cost nanocomposite solar cell. Further investigation is underway to optimize the PSC fabrication condition with these polymers for even better performances.

4. Experimental Section

4.1. General Measurement and Characterization. All chemicals are purchased from Aldrich and used as received unless otherwise specified. Compound **1** and diethyl 2,5-di-(2-thienyl)terephthalate (**2**) were synthesized according to the literature method.[12] 1-Bromo-4-*n*-hexylbenzene was obtained from Alfa Aesar Co. and used without further purification. ^{1}H and ^{13}C NMR spectra were measured using Bruker 400 MHz and Varian 200 MHz or 500 MHz instrument spectrometers. Thermal transitions were measured on PerkinElmer Instruments, differential scanning calorimeter (DSC)-TAC 7/DX and thermogravimetric analysis (TGA)-TGA 7 under a nitrogen atmosphere at a heating rate of 10 °C/min. Absorption spectra were taken on a PerkinElmer Lambda 950 UV−vis spectrophotometer. The molecular weight of polymers was measured by the GPC method (Waters), and polystyrene was used as the standard (THF as the eluent). The electrochemical cyclic voltammetry was conducted on an Autolab 5 voltammetric analyzer. A Pt plate coated with a thin polymer film was used as the working electrode and an $Ag/AgNO_3$ as the reference electrode, while 0.1 M tetrabutylammonium hexafluorophosphate ($TBAPF_6$) in acetonitrile was the electrolyte. CV curves were calibrated using ferrocence as the standard, whose HOMO is set at −4.8 eV with respect to zero vacuum level. The current−voltage ($I-V$) measurement of the PSC devices was conducted by a computer-controlled Keithley 2400 source measurement unit (SMU) with a Peccell solar simulator under the illumination of AM 1.5, 100 mW/cm^2. The illumination intensity was calibrated by a standard Si reference cell with KG-5 filter. The morphology of the polymer films was also analyzed by atomic force microscopy (AFM; VEECO DICP-II) with the dynamic force mode at ambient temperature. An etched Si probe under resonant frequency of 131 kHz and spring constants of 11 N/m was used.

4.2. Fabrication of Polymer Solar Cells. All the bulk-heterojunction photovoltaic cells were prepared using the same preparation procedures and device fabrication procedure as follows: the glass−indium tin oxide (ITO) substrates (obtained from Sanyo, Japan (8 Ω/□)) were first patterned by lithograph, then cleaned with detergent, and ultrasonicated in acetone and isopropyl alcohol, subsequently dried on hot plate at 120 °C for 5 min, and finally treated with oxygen plasma for 5 min. Poly(3,4-ethylenedioxythiophene):poly(styrenesulfonate) (PEDOT:PSS, Baytron P VP AI4083) was filtered through a 0.45 μm filter before being deposited by spin coating at 3000 rpm on ITO with a thickness of ∼30 nm in air, and removed to

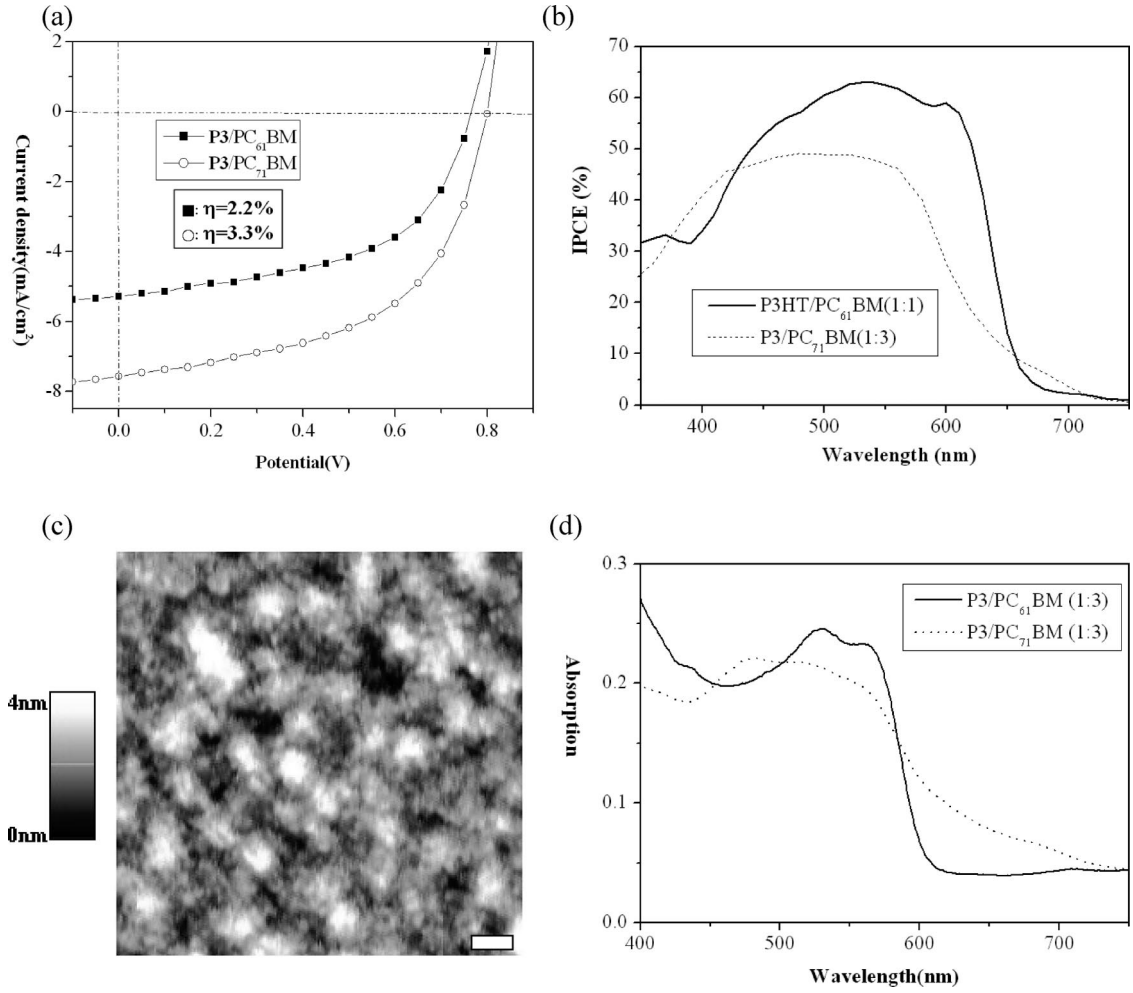

Figure 8. (a) Current density−potential characteristic of **P3**/PCBM solar cells devices under illumination with AM 1.5G solar simulated light ($PC_{61}BM$ (■) and $PC_{71}BM$ (○)). (b) The incident photon-to-current conversion efficiency (IPCE) spectra of devices fabricated with **P3HT**/$PC_{61}BM$ and **P3**/$PC_{71}BM$ system. (c) Topography image (size 1 μm × 1 μm; scale bar: 100 nm) obtained by tapping-mode AFM on the surface for **P3**/$PC_{71}BM$ (1:3) thin film. (d) Optical spectra of a **P3**/$PC_{61}BM$ blend film (thicker black line) and a **P3**/$PC_{71}BM$ film on glass.

glovebox to further dry at 150 °C for 30 min. The thin films of a blend of polymer/PCBM (1:2 or 1:3 w/w) were made by spin coating from 450 to 1500 rpm on the top of PEDOT:PSS layer from 10 mg/mL dichlorobenzene solution. After that, the device was annealed at 140 °C for 20 min in a glovebox. Subsequently, the device was completed by depositing 20 nm thickness of Ca and a 100 nm thickness of Al under $<10^{-6}$ torr pressure. The active area of the device is 4 mm^2.

4.3. Characterization of Field Effect Mobility of Polymer. Bottom-contact geometry was used to fabricate the thin-film field effect transistors.[13] A thermal oxide layer with a thickness of 100 nm was grown in a furnace on an N++ type low-resistance wafer which acts as a common gate electrode. Pt metal was used as source and drain electrodes, while their region were defined using photolithography process. The devices have a channel width of 1000 μm and channel length of 10 μm. Thin films of polymers were made by spin-coating a 1.0 wt % $CHCl_3$ or *o*-dichlorobenzene solution onto modified SiO_2 surface and dried for 1 h at 150 °C hot plate in a vacuum condition. Electric measurements were performed at room temperature in air by using semiconductor parameter analyzer (4156C, Agilent).

4.4. Synthetic Procedures. *Synthesis of Compound S1 (MTPT).* Compound **1** (626 mg, 1 mmol) and NBS (392 mg, 2.2 mmol) were dissolved in 20 mL chloroform. The reaction mixture was stirred under dark for 12 h. The solution was extracted with chloroform and washed with brine. The chloroform solution was dried over magnesium sulfate. Recrystallization from methanol afforded a light yellow product (88%). ^{1}H NMR ($CDCl_3$, 200 MHz) δ 7.29 (s, 2H), 7.05−7.12 (m, 16H), 6.94 (s, 2H), 2.29 (s, 12H). ^{13}C NMR ($CDCl_3$, 50 MHz) δ 155.1, 152.8, 141.4, 140.7, 135.9, 134.7, 128.6, 127.5, 127.2, 122.6, 117.1, 117.0, 62.6, 21.4.

Synthesis of Compound 4. To a solution of compound **2** (3.2 g, 8.3 mmol) in dry THF (20 mL) was added dropwisely 4-*n*-hexylphenyl magnesium bromide which was prepared in advance from 1-bromo-4-*n*-hexylbenzene (10.2 mL, 50.0 mmol) and magnesium turnings (1.2 g, 50.0 mmol). After refluxing overnight, the reaction mixture was quenched with water, extracted with ethyl acetate, and dried over magnesium sulfate. For removal of solvent, the crude product (**3**) was directly dissolved in acetic acid (100 mL) and then 5 mL of H_2SO_4 was added. The mixture was refluxed for 4 h and cooled. The reaction mixture was extracted with ethyl acetate and dried over magnesium sulfate. The solvent was evaporated under reduced pressure to give the crude product, which was purified by silica gel chromatography (hexanes as the eluent) to afford **4** as a yellow solid (3.2 g, 42%). ^{1}H NMR ($CDCl_3$, 200 MHz) δ 7.42 (s, 2H), 7.23 (d, J = 4.8 Hz, 2H), 7.09 (dd, J = 14.0, 8.0 Hz, 16H), 6.99 (d, J = 5.2 Hz, 2H), 2.54 (t, J = 8.0 Hz, 8H), 1.76 (m, 8H), 1.27−1.29 (m, 24H), 0.87 (t, J = 6.6 Hz, 12H). ^{13}C NMR ($CDCl_3$, 50 MHz) δ 155.2, 152.8, 141.3, 140.7, 135.8, 134.7, 128.6, 127.5, 127.3, 122.6, 117.1, 117.0, 62.5, 35.5, 32.3, 31.8, 22.6, 14.0. Anal. Calcd. for $C_{64}H_{74}S_2$: C, 84.71; H, 8.22.

Found: C, 84.31; H, 8.19.

Synthesis of Compound S2 (HTPT). Compound **4** (907 mg, 1 mmol) and NBS (392 mg, 2.2 mmol) were dissolved in 30 mL of chloroform. The reaction mixture was stirred under dark for 12 h. The solution was extracted with chloroform and washed with brine. The chloroform solution was dried over magnesium sulfate. Recrystallization from methanol afforded a light yellow product (92%). ^{1}H NMR ($CDCl_3$, 200 MHz) δ 7.32 (s, 2H), 7.07−7.09 (m, 16H), 6.99 (s, 2H), 2.56 (t, J = 8.0 Hz, 8H), 1.57 (m, 8H), 1.29 (m, 24H), 0.87 (t, J = 6.6 Hz, 12H). ^{13}C NMR ($CDCl_3$, 50 MHz) δ 155.1, 152.8, 141.4, 140.7, 135.9, 134.7, 128.6, 127.5, 127.2, 122.6, 117.1, 117.0, 62.6, 35.5, 32.3, 31.7, 22.6, 14.1. Anal. Calcd. for $C_{64}H_{72}Br_2S_2$: C, 72.16; H, 6.81. Found: C, 71.87; H, 6.43.

Synthesis of TPT Polymer P1. To a glass vial was added to **S1** (118 mg, 0.15 mmol), 5,5′-Bistrimethylstannyl-4,4′-bis(decyl)-2,2′-bithiophene (76 mg, 0.15 mmol), tris(dibenzylideneacetone)dipalladium(0) (5.5 mg, 2 mol %), tri(*o*-tolyl)phosphine (14.6 mg, 16 mol %), and chlorobenzene (5 mL), then degassed thrice via a freeze−pump−thaw cycle. The glass vial was placed into a microwave reactor and the mixture was reacted for 30 min. After polymerization, the dark solution was poured into methanol (1 L), and the black precipitate was collected on a membrane filter. The product was then subsequently washed by Soxhlet extractions for 72 h with methanol, acetone, and hexane. Finally, the polymer was dissolved in warm chloroform, precipitated, and filtered in methanol. The polymer was collected by centrifugation and dried under vacuum to obtain 0.1 g of **P1** (83% yield). GPC (THF): M_w 25 200 g/mol, λ_{max} = 490 nm (solid film). ^{1}H NMR ($CDCl_3$): δ = 7.4 (m, 2H of MTPT and 4H of bithiophene), δ = 7.0−7.2 (m, 18H, Ar−H of MTPT), δ = 2.54 (m, 4H), δ = 2.3 (m, 12H), δ = 1.76 (m, 4H), δ =1.27−1.29 (m, 24H), δ = 0.87 (t, 12H).

Synthesis of TPT Polymer P2. The polymerization of **S2** was carried out as follows: to a solution of $Ni(COD)_2$ (0.53 g, 1.9 mmol) in 15 mL of dry *N*,*N*-dimethylformamide (DMF) was added 0.35 mL of 1,5-cyclooctadiene and 2,2′-bipyridyl (0.30 g, 1.9 mmol) under N_2. Then, a solution of **S2** (0.44 g, 1.6 mmol) in 10 mL of mixing solvent (DMF/toluene) was added, and the former mixture was stirred at 60 °C for 48 h. The reaction mixture was poured into aqueous ammonia to obtain an orange precipitate, which was washed with NH_4OH (aq) (3 times), toluene (once), a warm aqueous solution of disodium ethylenediaminetetraacetate (3 times), aqueous ammonia, warm water, and toluene (once). The powder was collected by filtration and dried under vacuum to obtain **P2**. GPC (THF): M_w 21 800 g/mol, λ_{max} = 510 nm (solid film). ^{1}H NMR ($CDCl_3$): δ = 7.4 (m, 2H of HTPT), δ = 7.0−7.2 (m, 18H, Ar−H of HTPT), δ = 2.54 (m, 8H), δ = 1.76 (m, 8H), δ =1.27−1.29 (m, 24H), δ = 0.87 (t, 12H).

Synthesis of TPT Polymer P3. The copolymer **P3** was prepared by a procedure similar to that of **P1** by using **S2** and 2, 5-bis(trimethylstannyl)thiophene as the monomers to yield 0.14 g of the product. (94% yield). GPC (THF): M_w 48 700 g/mol, λ_{max} = 510 nm (solid film). ^{1}H NMR ($CDCl_3$): δ = 7.4 (m, 2H of HTPT and 2H of thiophene), δ = 7.0−7.2 (m, 18H, Ar−H of HTPT), δ = 2.54 (m, 8H), δ = 1.76 (m, 8H), δ =1.27−1.29 (m, 24H), δ = 0.87 (t, 12H).

Synthesis of TPT Polymer P4. The copolymer **P4** was prepared by the procedure similar to that of **P1** by using **S2** and 5,5′-bis(trimethylstannyl)[2,2′]bithiophene as the monomers to afford 0.11 g of the product (68% yield). GPC (THF): M_w 29 300 g/mol, λ_{max} = 508 nm (solid film). ^{1}H NMR ($CDCl_3$): δ = 7.4 (m, 2H of HTPT and 4H of bithiophene), δ = 7.0−7.2 (m, 18H, Ar−H of HTPT), δ = 2.54 (m, 8H), δ = 1.76 (m, 8H), δ =1.27−1.29 (m, 24H), δ = 0.87 (t, 12H).

Acknowledgment. The authors thank the Ministry of Economic Affairs, Taiwan, for financially supporting this research.

References and Notes

(1) (a) Brabec, C. J.; Sariciftci, N. S.; Hummelen, J C. *Adv. Funct. Mater.* **2001**, *11*, 15. (b) Spanggaard, H.; Krebs, F. C. *Sol. Energy Mater. Sol. Cells* **2004**, *83*, 125. (c) Coakley, K. M.; McGehee, M. D. *Chem. Mater.* **2004**, *16*, 4533. (d) Hoppea, H.; Sariciftci, N. S. *J. Mater. Res.* **2004**, *19*, 1924. (e) Gunes, S.; Neugebauer, H.; Sariciftci, N. S. *Chem. Rev.* **2007**, *107*, 1324.

(2) Yu, G.; Gao, J.; Hemmelen, J. C.; Wudl, F.; Heeger, A. J. *Science* **1995**, *270*, 1789.

(3) (a) Ma, W.; Yang, C.; Gong, X.; Lee, K.; Heeger, A. J. *Adv. Funct. Mater.* **2005**, *15*, 1617–1622. (b) Kim, J. Y.; Kim, S. H.; Lee, H. H.; Lee, K.; Ma, W.; Gong, X.; Heeger, A. J. *Adv. Mater.* **2006**, *18*, 572–576. (c) Li, G.; Shrotriya, V.; Huang, J.; Yao, Y.; Moriarty, T.; Emery, K.; Yang, Y. *Nat. Mater.* **2005**, *4*, 864–868. (d) Kim, J. Y.; Lee, K.; Coates, N. E.; Moses, D.; Nguyen, T.-Q.; Dante, M.; Heeger, A. J. *Science* **2007**, *317*, 222.

(4) (a) Winder, C.; Sariciftci, N. S. *J. Mater. Chem.* **2004**, *14*, 1077. (b) Bundgaard, E.; Krebs, F. C. *Sol. Energy Mater. Sol. Cells* **2007**, *91*, 954. (c) Hou, J. H.; Tan, Z. A.; Yan, Y.; He, Y. J.; Yang, C. H.; Li, Y. F. *J. Am. Chem. Soc.* **2006**, *128*, 4911.

(5) (a) Miyakoshi, R.; Yokoyama, A.; Yokozawa, T. *Macromol. Rapid Commun.* **2004**, *25*, 1229. (b) Schilinsky, P.; Asawapirom, U.; Scherf, U.; Biele, M.; Brabec, C. *J. Chem. Mater.* **2005**, *17*, 2175.

(6) (a) Yamamoto, T.; Komarudin, D.; Arai, M.; Lee, B.-L.; Suganuma, H.; Asakawa, N.; Inoue, Y.; Kubota, K.; Sasaki, S.; Fukuda, T.; Matsuda, H. *J. Am. Chem. Soc.* **1998**, *120*, 2047. (b) Sirringhaus, H.; Brown, P. J.; Friend, R. H.; Nielsen, M. M.; Bechgaard, K.; Langeveld-Voss, B. M. W.; Spiering, A. J. H.; Janssen, R. A. J.; Meijer, E. W.; Herwig, P.; de Leeuw, D. W. *Nature (London)* **1999**, *401*, 685. (c) Osterbacka, R.; An, C. P.; Jiang, X. M.; Vardeny, Z. V. *Science* **2000**, *287*, 839.

(7) McCulloch, I.; Heeney, M.; Bailey, C.; Genevicius, K.; Macdonald, I.; Shkunov, M.; Sparrowe, D.; Tierney, S.; Wagner, R.; Zhang, W. M.; Chabinyc, M. L.; Kline, R. J.; McGehee, M. D.; Toney, M. F. *Nat. Mater.* **2006**, *5*, 328.

(8) Osaka, I.; Sauvé, G.; Zhang, R.; Kowalewski, T.; McCullough, R. D. *Adv. Mater.* **2007**, *19*, 4160–4165.

(9) (a) Pan, H.; Wu, Y.; Li, Y.; Liu, P.; Ong, B. S.; Zhu, S.; Xu, G. *Adv. Funct. Mater.* **2007**, *17*, 3574–3579. (b) Pan, H.; Li, Y.; Wu, Y.; Liu, P.; Ong, B. S.; Zhu, S.; Xu, G. *J. Am. Chem. Soc.* **2007**, *129*, 4112–4113.

(10) (a) Ando, S.; Nishida, J.; Inoue, Y.; Tokito, S.; Yamashita, Y. *J. Mater. Chem.* **2004**, *14*, 1787. (b) Ando, S.; Nishida, J.; Fujiwara, E.; Tada, H.; Inoue, Y.; Tokito, S.; Yamashita, Y. *Chem. Lett.* **2004**, 1170. (c) Ando, S.; Nishida, J.; Tada, H.; Inoue, Y.; Tokito, S.; Yamashita, Y. *J. Am. Chem. Soc.* **2005**, *127*, 5336.

(11) Zhang, R.; Li, B.; Iovu, M. C.; Jeffries-EL, M.; Sauvé, G.; Cooper, J.; Jia, S.; Tristram-Nagle, S.; Smilgies, D. M.; Lambeth, D. N.; McCullough, R. D.; Kowalewski, T. *J. Am. Chem. Soc.* **2006**, *128*, 3480.

(12) Wong, K.-T.; Chao, T.-C.; Chi, L.-C.; Chu, Y.-Y.; Balaiah, A.; Chiu, S.-F.; Liu, Y.-H.; Wang, Y. *Org. Lett.* **2006**, *8*, 5033–5036.

(13) (a) Babel, A.; Jenekhe, S. A. *J. Am. Chem. Soc.* **2003**, *125*, 13656. (b) Zhu, Y.; Babel, A.; Jenekhe, S. A. *Macromolecules* **2005**, *38*, 7983. (c) Babel, A.; Jenekhe, S. A. *Macromolecules* **2003**, *36*, 7759. (d) Zhu, Y.; Champion, R. D.; and Jenekhe, S. A. *Macromolecules* **2006**, *39*, 8712–8719. (e) Yasuda, T.; Sakai, Y.; Aramaki, S.; Yamamoto, T. *Chem. Mater.* **2005**, *17*, 6060–6068.

(14) Gur, I.; Fromer, N. A.; Chen, C.-P.; Kanaras, A. G.; Alivisatos, A. P. *Nano Lett.* **2007**, *7*, 409–414.

(15) (a) Shaheen, S. E.; Brabec, C. J.; Sariciftci, N. S.; Padinger, F.; Fromherz, T.; Hummelen, J. C. *Appl. Phys. Lett.* **2001**, *78*, 841–843. (b) Wienk, M. M.; Kroon, J. M.; Verhees, W. J. H.; Knol, J.; Hummelen, J. C.; Van Hal, P. A.; Janssen, R. A. J. *Angew. Chem., Int. Ed.* **2003**, *42*, 3371–3375.

MA800494K